SUPPORTING INFORMATION

Magnetic imaging of domain walls in the antiferromagnetic topological insulator $MnBi_2Te_4$

Paul M. Sass[†], Wenbo Ge[†], Jiaqiang Yan[‡], D. Obeysekera[§], J.J Yang[§], and Weida Wu[†,].*

[†] Department of Physics and Astronomy, Rutgers University, Piscataway, NJ 08854, USA.

[‡] Materials Science and Technology Division, Oak Ridge National Laboratory, Oak Ridge, Tennessee 37831, USA.

[§] Department of Physics, New Jersey Institute of Technology, Newark, 07102 USA

*wdwu@physics.rutgers.edu

Note 1: *in-situ* transport data for constructing *H*-*T* phase diagrams

The *H*-*T* phase diagrams of $MnSb_2Te_4$, $MnBi_{1.37}Sb_{0.63}Te_4$, $MnBi_2Te_4$ and $EuMnBi_2$ crystals are constructed from resistance anomalies measured by in-situ transport.

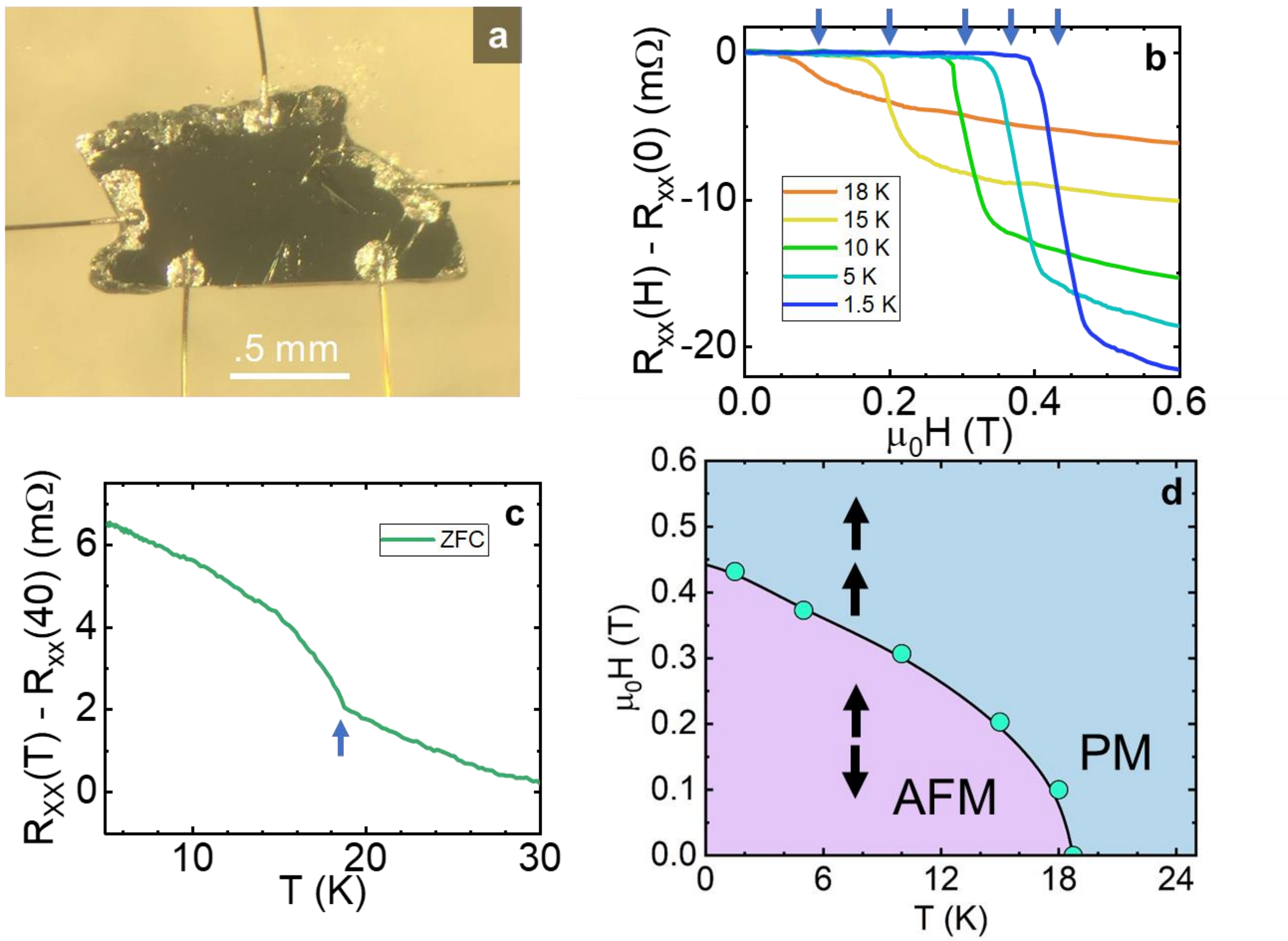

Figure S1. (a) Optical image of MST single crystal with Au wires for in-situ transport measurements. (b,c) Longitudinal resistance versus applied field and temperature used to complete the *H*-*T* phase diagram (d). The blue arrows indicate AFM transition. The current used for transport measurement was 100 μA.

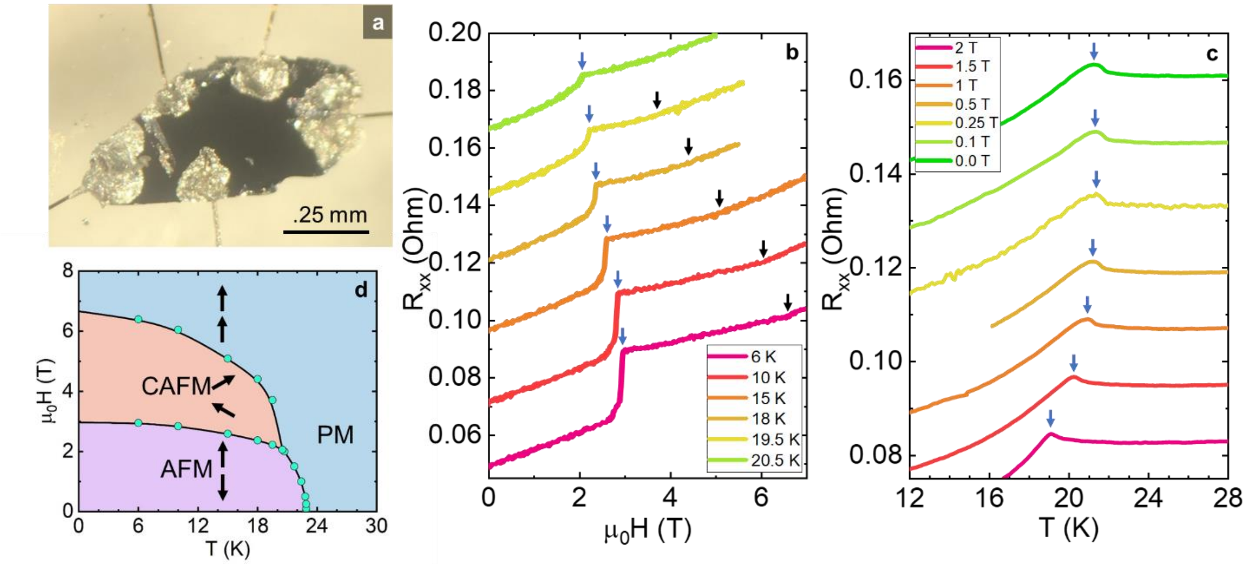

Figure S2. (a) Optical image of MBST single crystal. (b,c) Longitudinal resistance versus applied field and temperature used to complete the *H*-*T* phase diagram (d). The small blue (black) arrows indicate AFM to PM or AFM to CAFM (CAFM to PM) transition. The current used for transport was 200 μA.

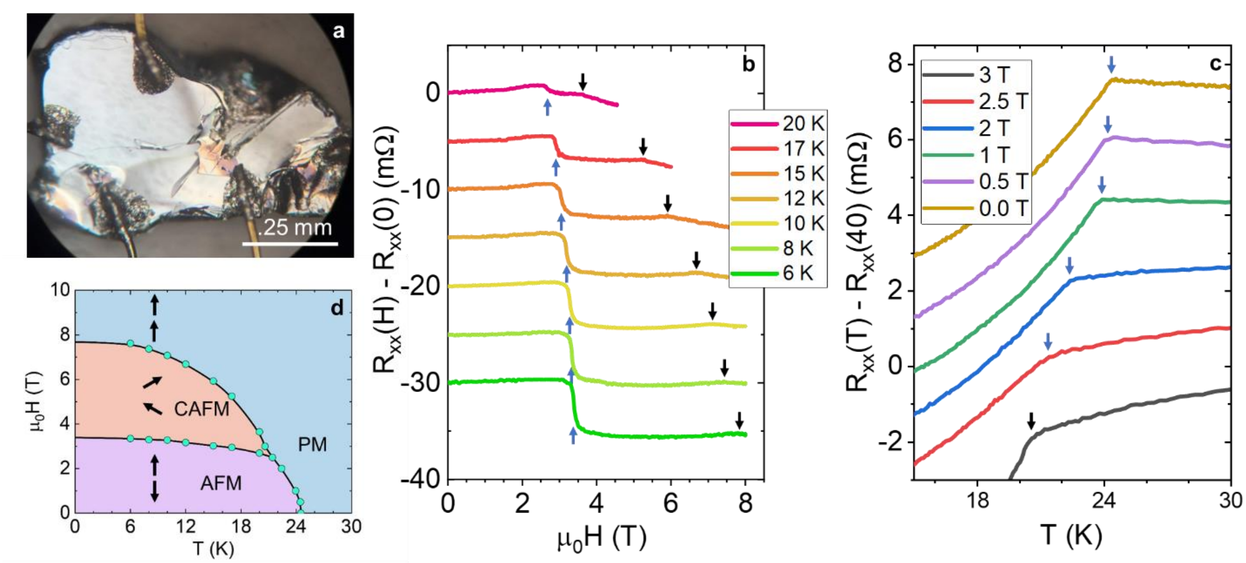

Figure S3. (a) Optical image of MBT single crystal with Au leads for Hall transport. (b,c) Longitudinal resistance versus applied field and temperature used to complete the *H*-*T* phase diagram (d). The small blue (black) arrows indicate AFM to PM or AFM to CAFM (CAFM to PM) transition. The current used for transport was 4 mA.

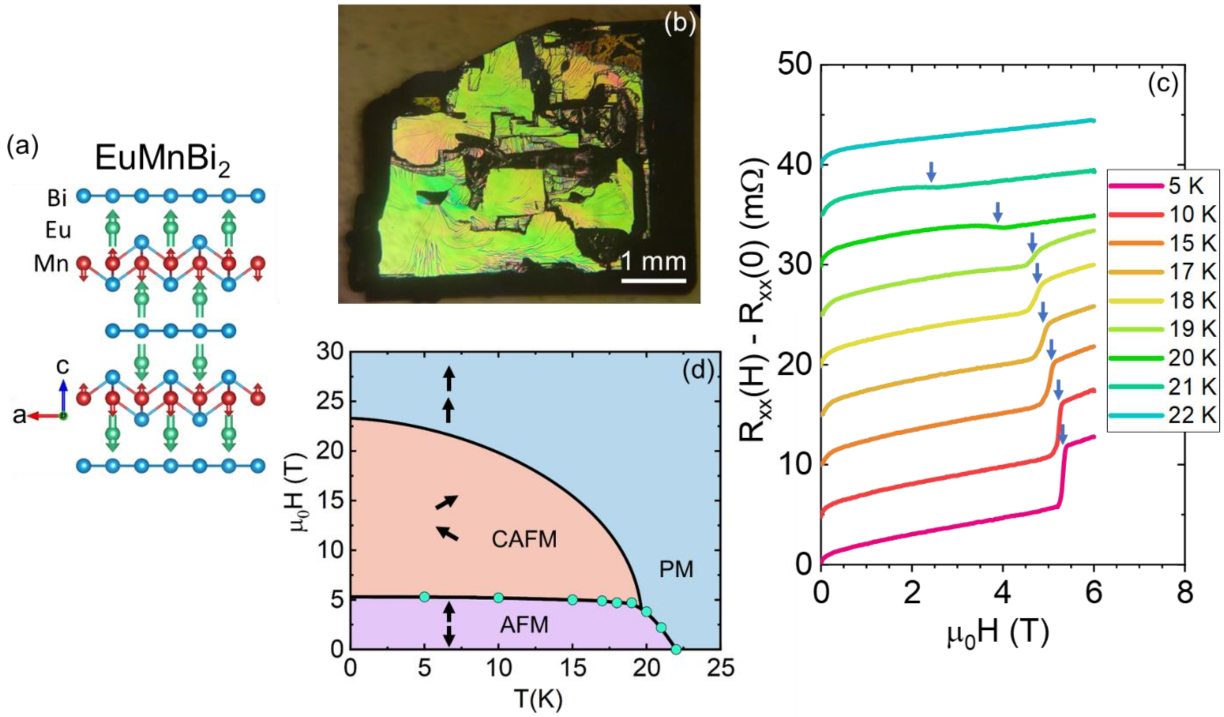

Figure S4. (a) A schematic illustration of crystal structure and magnetic order of $EuMnBi_2$. (b) Optical image of as-grown $EuMnBi_2$ single crystal (transport leads not shown). (c) Longitudinal resistance versus applied field and temperature used to complete the *H*-*T* phase diagram (d). The small blue arrows indicate AFM to CAFM or AFM to PM transition. The current used for transport was 100 μA.

Note 2: Temperature and Magnetic field dependence of domain wall contrast in $MnSb_2Te_4$, $MnBi_{1.37}Sb_{0.63}Te_4$, $MnBi_2Te_4$, and $EuMnBi_2$ single crystals.

Here we present complete data sets of field dependent MFM results of these antiferromagnets and the analysis of the domain wall contrast.

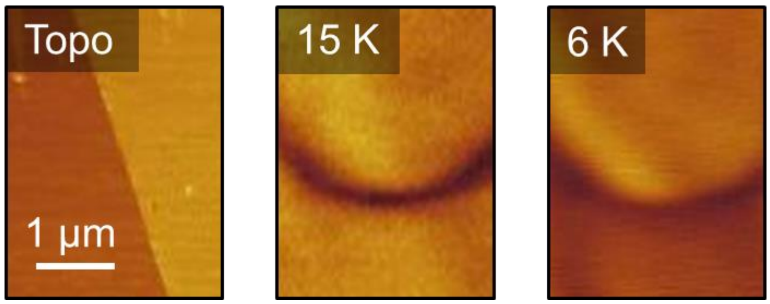

Figure S5. Topography and MFM images at 15 K and 6 K of $MnSb_2Te_4$, respectively. The 6 K MFM image shows clear domain contrast in addition to DW signal. The color scale for the topography and MFM images are 15 nm and 0.2 Hz.

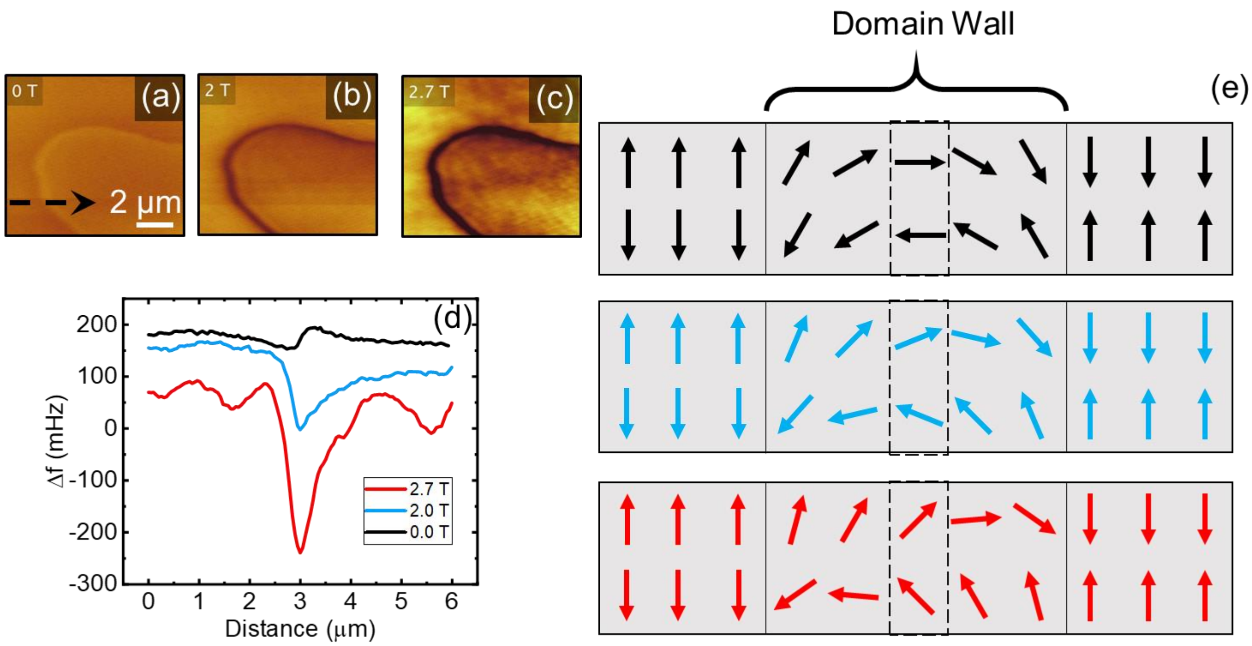

Figure S6. (a-c) MFM images from field sweep in Fig. S10 on $MnBi_2Te_4$. (d) Line profiles of the domain wall along the black dotted line in (a) at different magnetic fields showing a significant enhancement of domain wall contrast. (e) Spin configurations of domains and domain wall for each line profile in (d). The black spin configuration (0.0 T) has a DW in the spin-flop state, leading to a line profile that is more skewed. The blue and red spin configurations (2.0 and 2.7 T) however, have a DW with a net out-of-plane moment. This is due to the out-of-plane applied field staggering the parallel and anti-parallel moments, i.e. the anti-parallel moments are more easily rotated than the parallel moments. This leads to a stronger net moment in the DW and thus a stronger DW contrast. The color scale for the MFM images in 0.2 Hz.

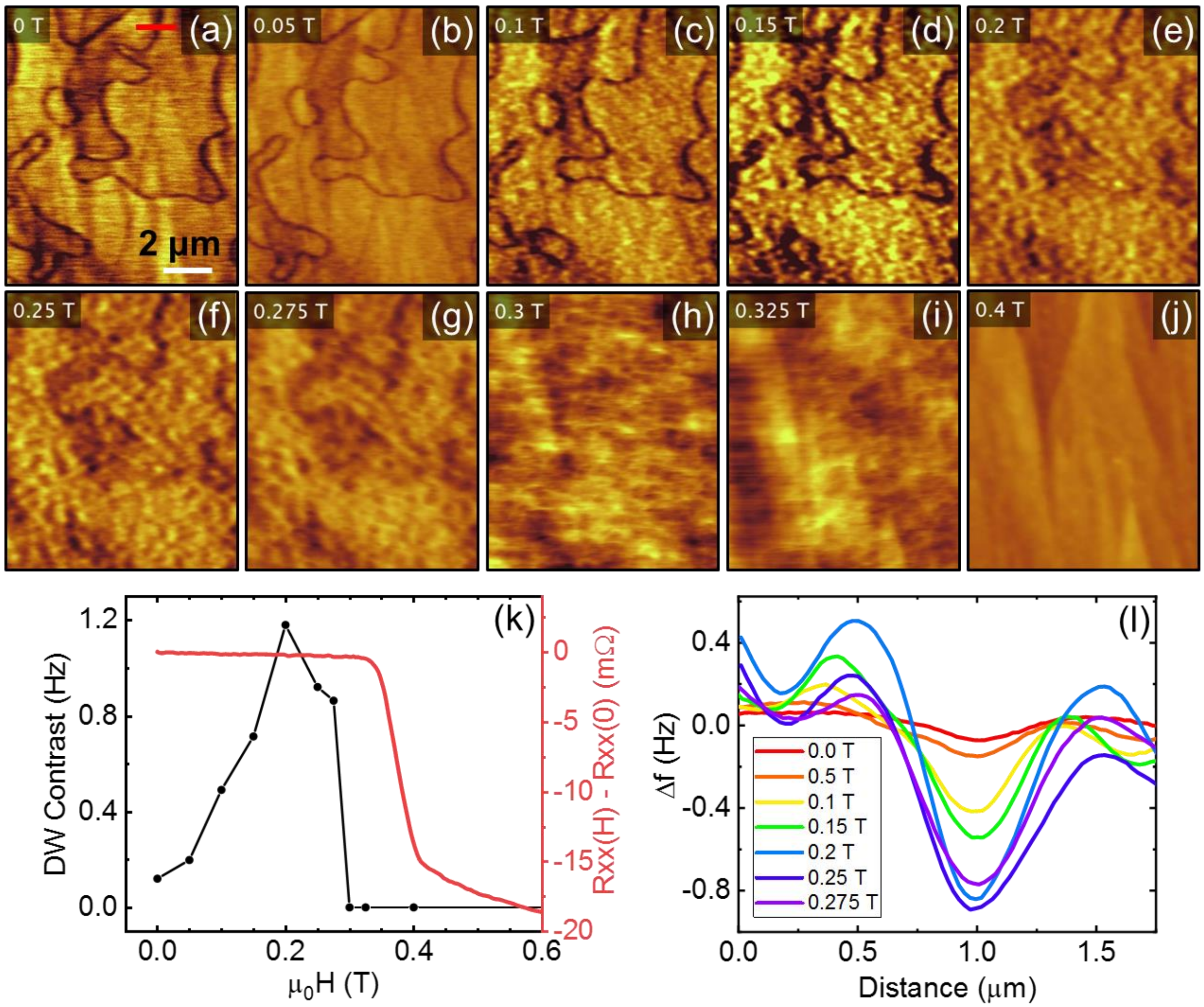

Figure S7. (a-j) Complete *H*-dependence MFM images of $MnSb_2Te_4$ at 5 K (some are shown in Figure 1)**.** DW contrast was measured on red line shown in (a). The observed DWs get weaker and fuzzy above 0.2 T, probably due to the stray field of MFM tip. DWs become unrecognizable as *H* approaches the spin-flip transition (~0.35 T), as shown in (h) and (i). No DWs are observed above the spin-flip transition at 0.4 T (j). This is in contrast to MBT and MBST. (k) *H*-dependence of DW contrast (black) and longitudinal resistance (red) on $MnSb_2Te_4$ single crystal. The contrast of the DWs increases up to 0.2 T, then decreases and becomes unmeasurable above 0.3 T (h, i). The onset of the spin-flip transition is ~0.35 T, which completes at ~0.4 T (j). The color scales for the MFM images are 0.2 (a), 1 (b-d) and 3 Hz (e-j). (l) Line profiles of the domain wall along the red line in (a) at different magnetic fields showing a significant enhancement of domain wall contrast.

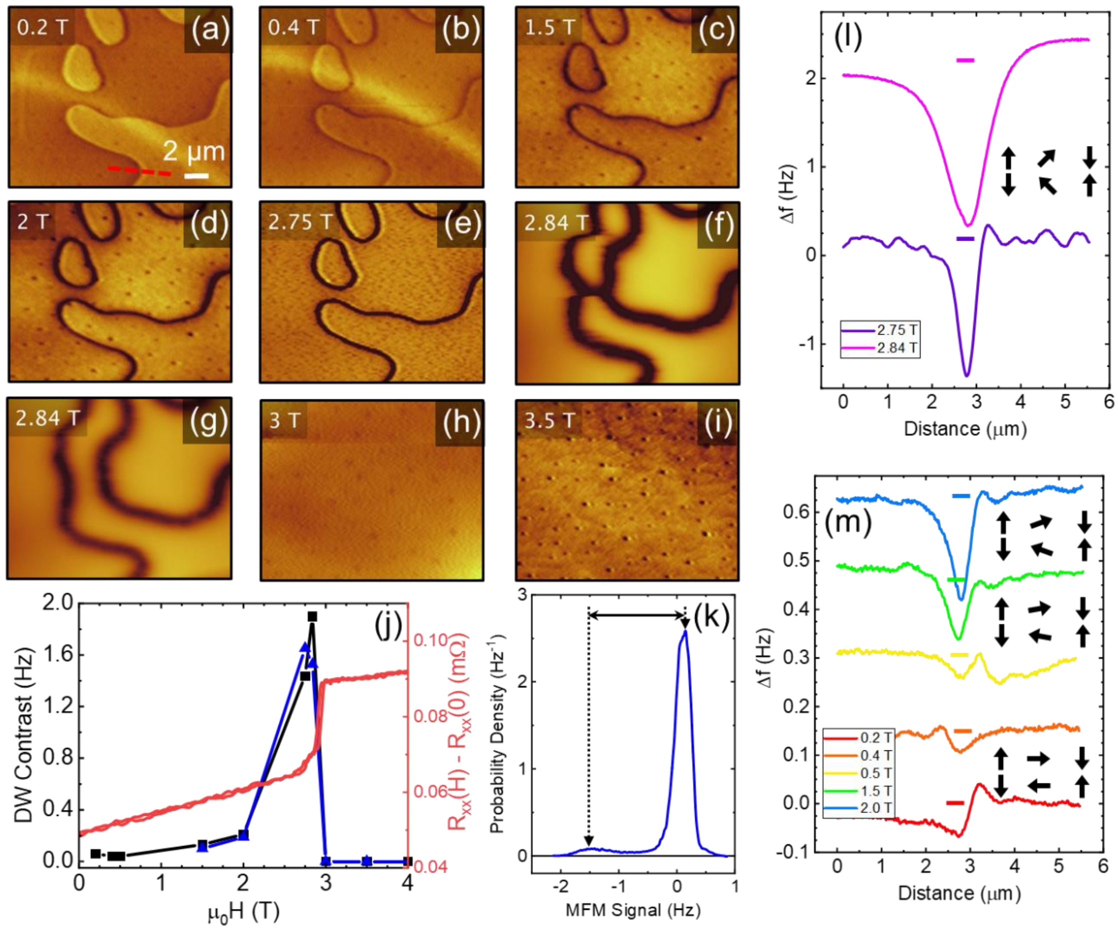

Figure S8. (a-i) Complete *H*-dependence of MFM images of $MnBi_{1.37}Sb_{0.63}Te_4$ at 6 K (some are shown in Figure 2) with 100 nm lift height. The DW contrast was measured on the red line shown in Figure 2a in the main text. The light bands in (a) and (b) are a scanning artifact. At 2.84 T (f), the DWs strongly interact with the MFM tip moment, resulting in domains coalescing. (see Figure S11 for another example). Increasing the lift height to 400 nm stabilizes MFM scanning, as shown in (g). This observation demonstrates the possibility of local manipulation of mobile AFM DWs. (j) *H*-dependence of DW contrast (black) and longitudinal resistance (red) on $MnBi_{1.37}Sb_{0.63}Te_4$ single crystal at 6 K. The contrast of the DWs increase linearly below 2 T, then rises sharply above 2 T up to the spin-flop transition (~2.87 T), then completely disappears at 3 T (h). The blue curve is the DW contrast extracted using a histogram of the MFM signal (an example is shown in (k)). It matches well to the DW contrast extracted using line profiles, suggesting that the DW contrast is uniform. (l, m) Line profiles of the domain wall along the red dotted line in (a) at different magnetic fields showing a significant enhancement of domain wall contrast. The short colored lines in the middle of the DWs indicate the baseline of the DW contrast. The baseline at low field

(< 1.5 T) is midway between peak and trough, since the domain contrast skews the baseline level. The DW moments (black arrows) are displayed to show how they evolve with applied field, leading to a stronger DW moment. The color scales for the MFM images are 0.3 (a-d), 2 (e-g) and 0.3 Hz (h, i).

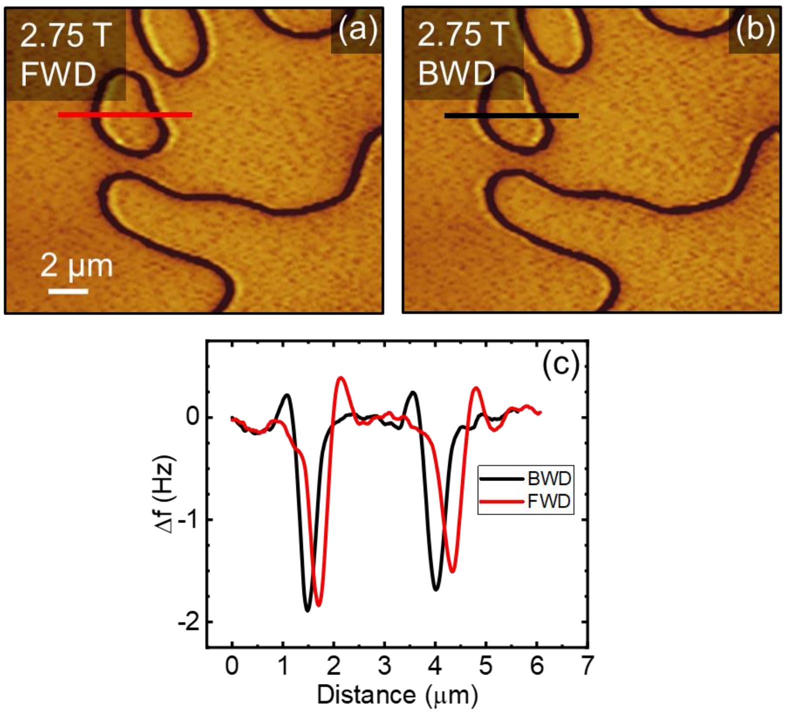

Figure S9. (a, b) MFM images at 2.75 T from Fig. 2 of $MnBi_{1.37}Sb_{0.63}Te_4$ with forward (FWD) and backward (BWD) scanning directions, respectively. (c) Line profiles of red and black lines in (a) and (b). The "shadowing" seen in the MFM images is symmetric between forward and backward scanning directions, and thus is not an intrinsic effect. The color scale for the MFM images is 2 Hz.

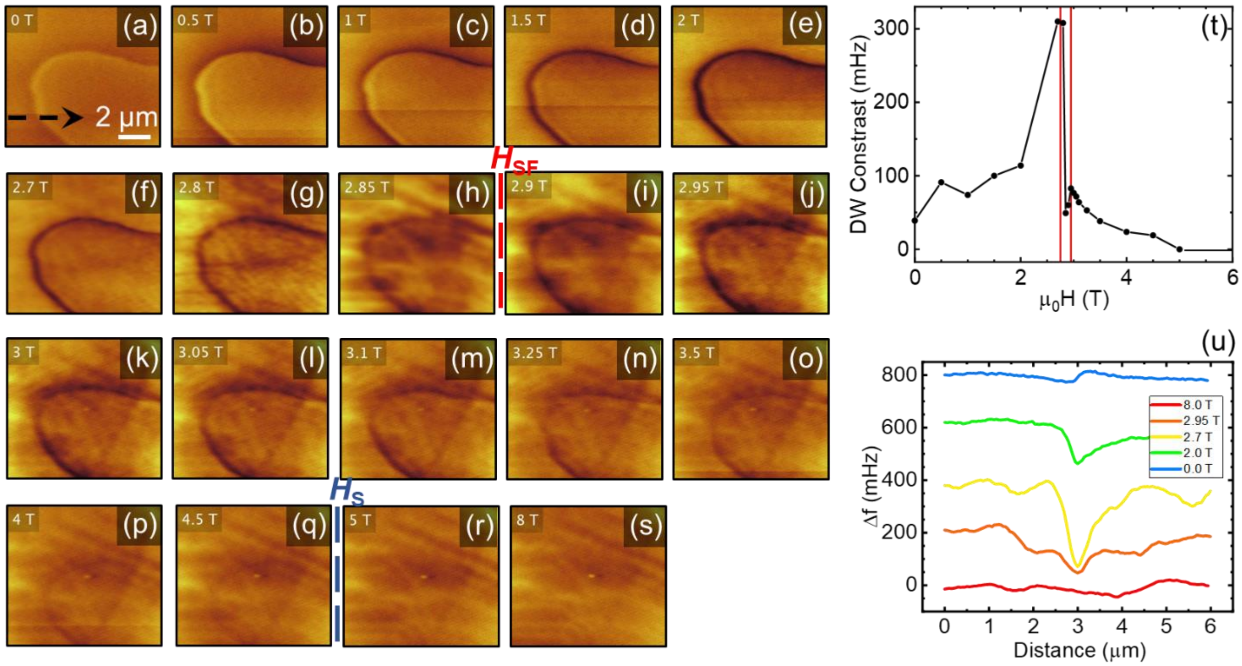

Figure S10. (a-s) Complete H-dependence of MFM images at 18 K on $MnBi_2Te_4$ single crystal (some are shown in Figure 3 in main text). The line profile (black dotted arrow) used for DW contrast analysis. (t) *H*-dependence of DW contrast (black) (18 K) vs applied field on $MnBi_2Te_4$ single crystal. The DW contrast increases approximately linearly with field up to 2 T, then rises quickly above 2 T up to the spin-flop transition (~2.87 T), then plummets down sharply at the transition. Above the spin-flop transition, the DW contrast decreases slowly in the CAFM state until the saturation transition at ~4.7 T, then disappears in the saturation state. (u) Line profiles of the domain wall along the black dotted line in (a) at different magnetic fields showing a significant enhancement of domain wall contrast. The color scales for the MFM images are 0.3 (a-e), 1 (f-h), 0.5 (i) and 0.3 Hz (j-s).

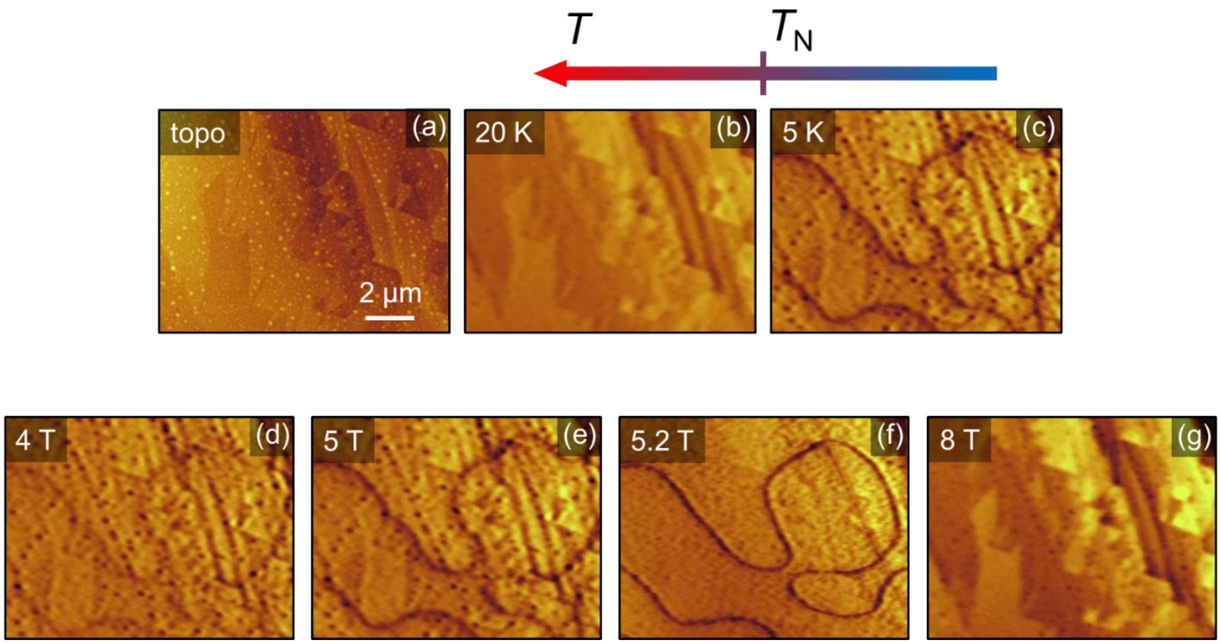

Figure S11. (a) Topographic image of as-grown $EuMnBi_2$ single crystal surface. (b,c) MFM images taken near and well below T_N (~ 22 K) at 5 T. No domain wall is visible above T_N. Below however, a curvilinear DW appears in the scan window. Contrast from the surface is visible at high field. (d-g) MFM images taken on the same location with increasing magnetic fields (labelled in the upper right corner) showing increasing contrast of curvilinear DW. The highest DW contrast is right before the spin-flop transition, above which (g) there is no DW contrast in view. The color scales for the topographic and MFM images are 40 nm (a) and 2 (b,g), 1 (c,d,e), 4 (f) Hz.

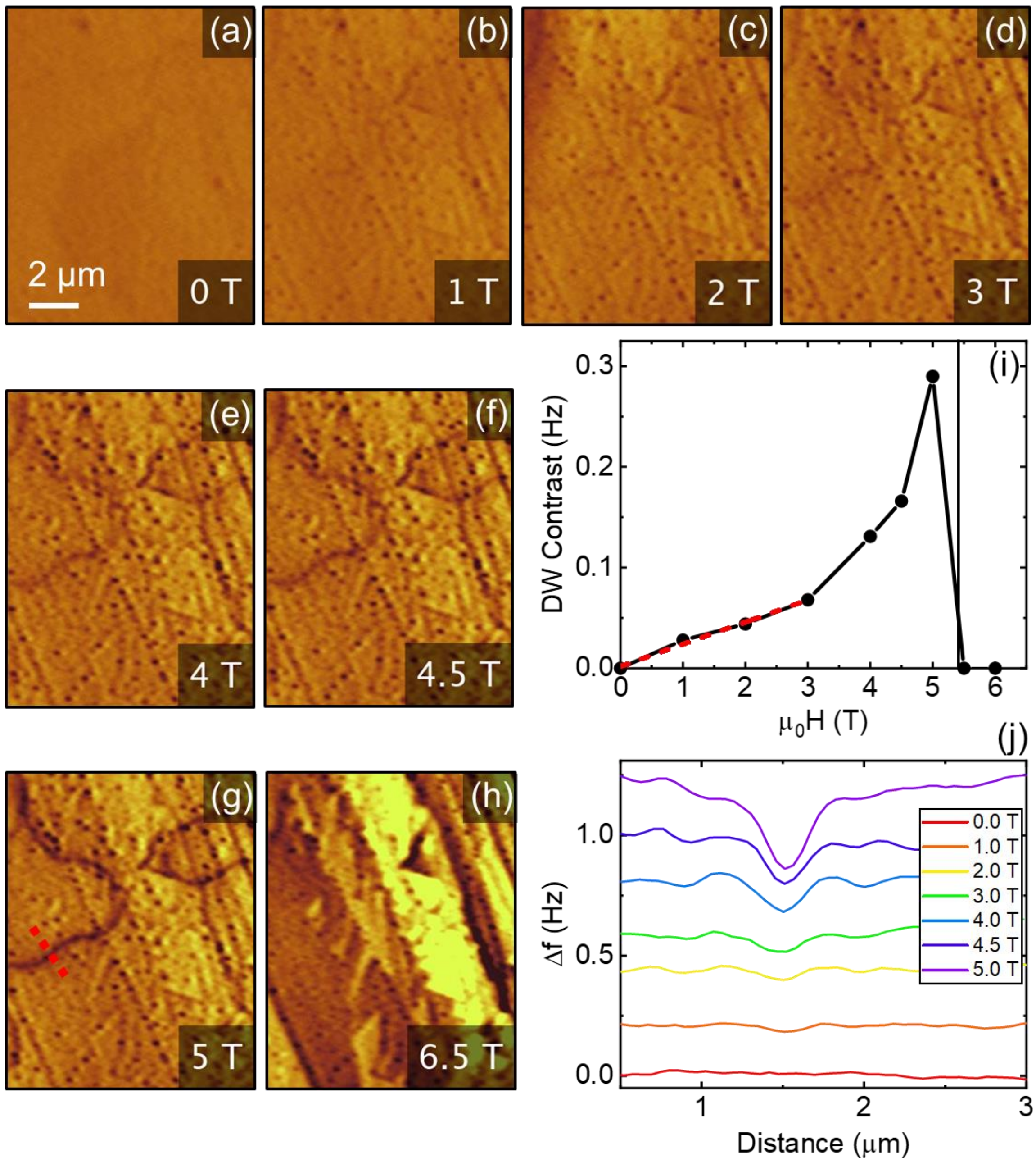

Figure S12. (a-h) MFM images taken after 50 mT FC on the same location with increasing magnetic fields (labelled in the lower right corner) showing increasing contrast of curvilinear DWs. (i) *H*-dependence of DW contrast on EMB single crystal extracted from red dotted line in (g). The DW contrast increases up to the spin-flop transition, labeled by black vertical line, then disappears above the transition. (l) Line profiles of the domain wall along the red dotted line in (g) at different magnetic fields showing a significant enhancement of domain wall contrast. The color scale for the MFM images 1 Hz.

Note 3: Estimation of domain wall width.

Here we use the formula for ferromagnetic domain wall width $\delta = \pi\sqrt{\frac{A}{K}}a$ to estimate the width of A-type AFM DW widths. Here A is the exchange stiffness energy constant, K is the anisotropy energy, and a is the lattice constant ($\approx$ 0.43 nm). A can be estimated from the ordering temperature T_N, $A \approx k_B T_N$. K can be estimated from the Zeeman energy at the spin-flop (spin-flip) transition, $K \approx M_{SF} H_{SF}/2$, because it is approximately the energy gain to overcome the anisotropy energy (*1*). Here M_{SF} is the magnetization value just above the spin-flop or spin-flip transition (which is **not** the saturation moment), and H_{SF} is the spin-flop or spin-flip transition field. The estimated domain wall widths are listed in Table T1.

Crystal	T_N	H_{SF}	M_{SF}	δ
$MnBi_2Te_4$	24 K	3.6 T	1.5 μ_B/Mn	5 nm
$MnBi_{1.37}Sb_{0.63}Te_4$	23 K	3.0 T	1.3 μ_B/Mn	6 nm
$MnSb_2Te_4$	19 K	0.4 T	1.5 μ_B/Mn	13 nm
$EuMnBi_2$	22 K	5.4 T	1.5 μ_B/Mn	4 nm

Table T1. The estimated DW widths of 4 – 13 nm are much different than the measured DW widths of ~500 nm. This is probably due to a combination of the diameter of the tip (100 – 200 nm) and the tip-sample distance ~ 50 – 100 nm. Therefore, the widths of the DWs are likely resolution limited.

Note 4: Domain wall creep and coalescence in $MnSb_2Te_4$, $MnBi_{1.37}Sb_{0.63}Te_4$, and $MnBi_2Te_4$.

Ramping magnetic field could cause domain wall creeping and coalescing in $MnSb_2Te_4$, $MnBi_{1.37}Sb_{0.63}Te_4$ and $MnBi_2Te_4$.

4.1 $MnSb_2Te_4$

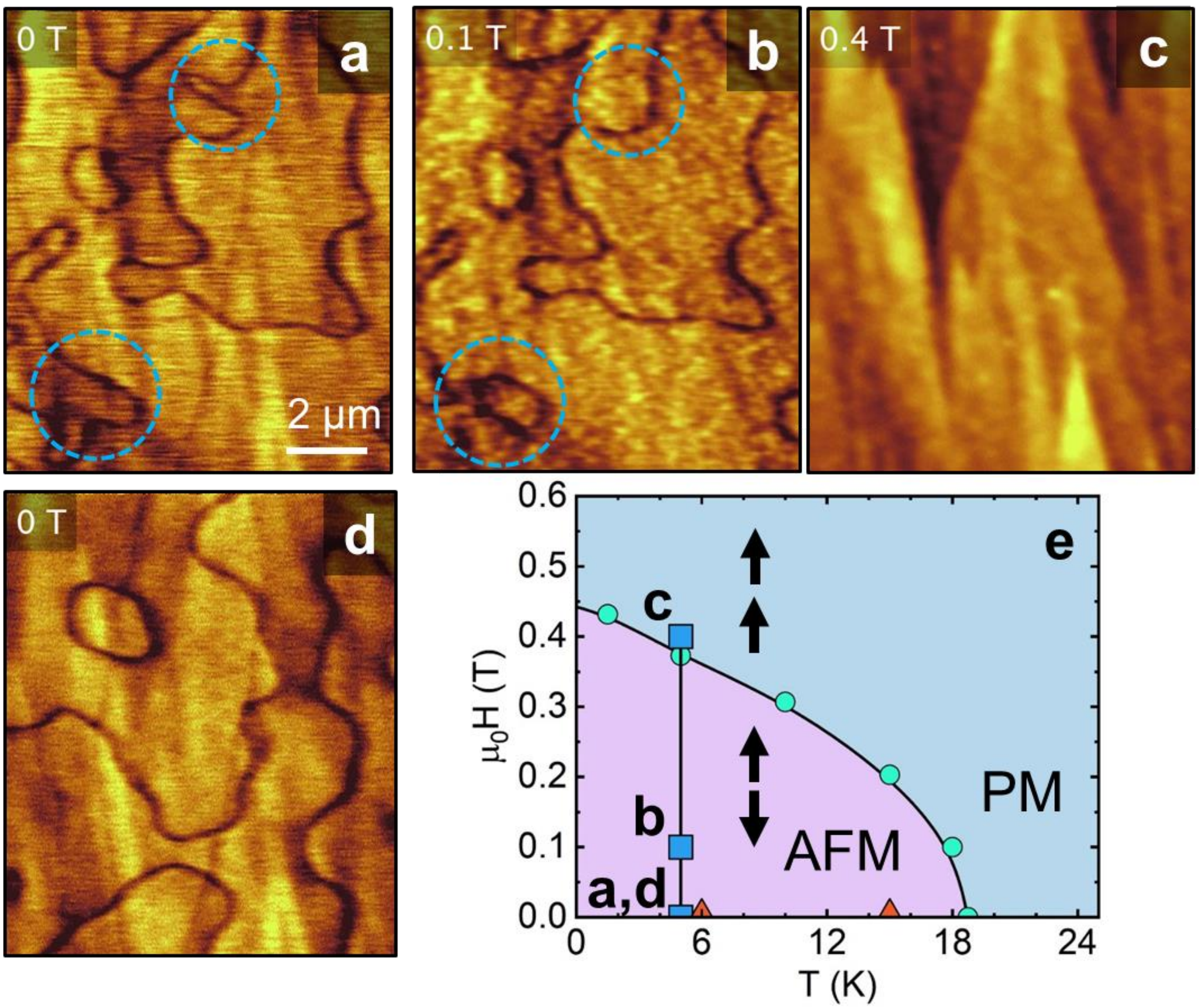

Figure S13. (a-d) MFM images of field cycle (5 K) taken at the same location after 0.15 T FC. The color scale is 1 and 0.3 Hz for (b,c) and (a,d). Cyan circles indicate creeps of DWs after applying 0.1 T. (e), Magnetic phase diagram showing the spin-flip transition from the A-type antiferromagnetic state to saturation state indicated by black arrows. Blue squares show the fields at which the images (a-d) are taken.

4.2 $MnBi_{1.37}Sb_{0.63}Te_4$

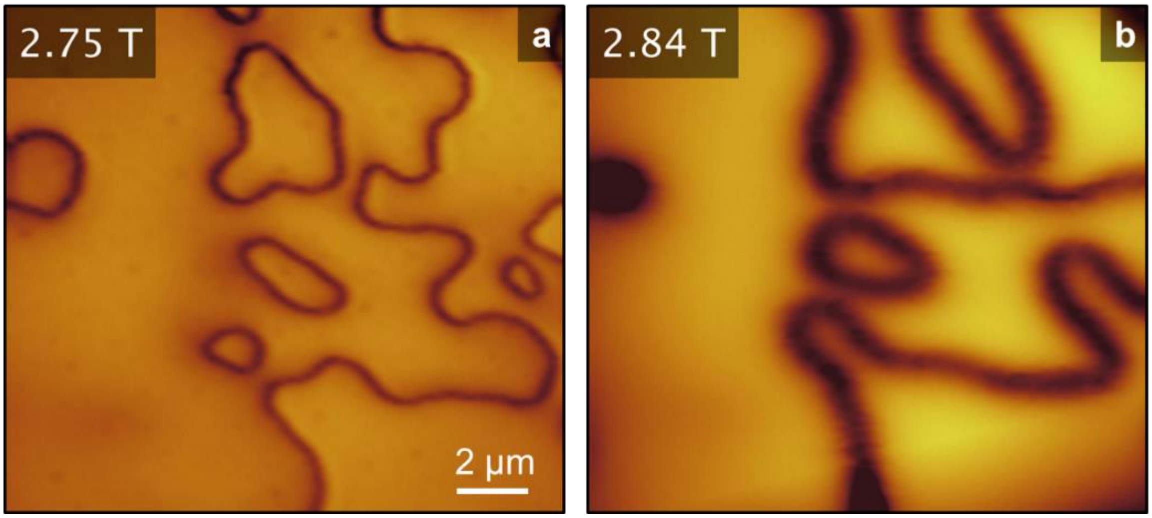

Figure S14. (a,b) MFM images at 6 K after 2 T field cooling. The domain configuration is stable until 2.75 T. At 2.84 T, DWs interact strongly with MFM tip stray field so that some domains merged (with DW annihilation). The strong interaction also results in broadened and fuzzy DWs. The color scale for the MFM images is 1.8 Hz.

4.3 $MnBi_2Te_4$

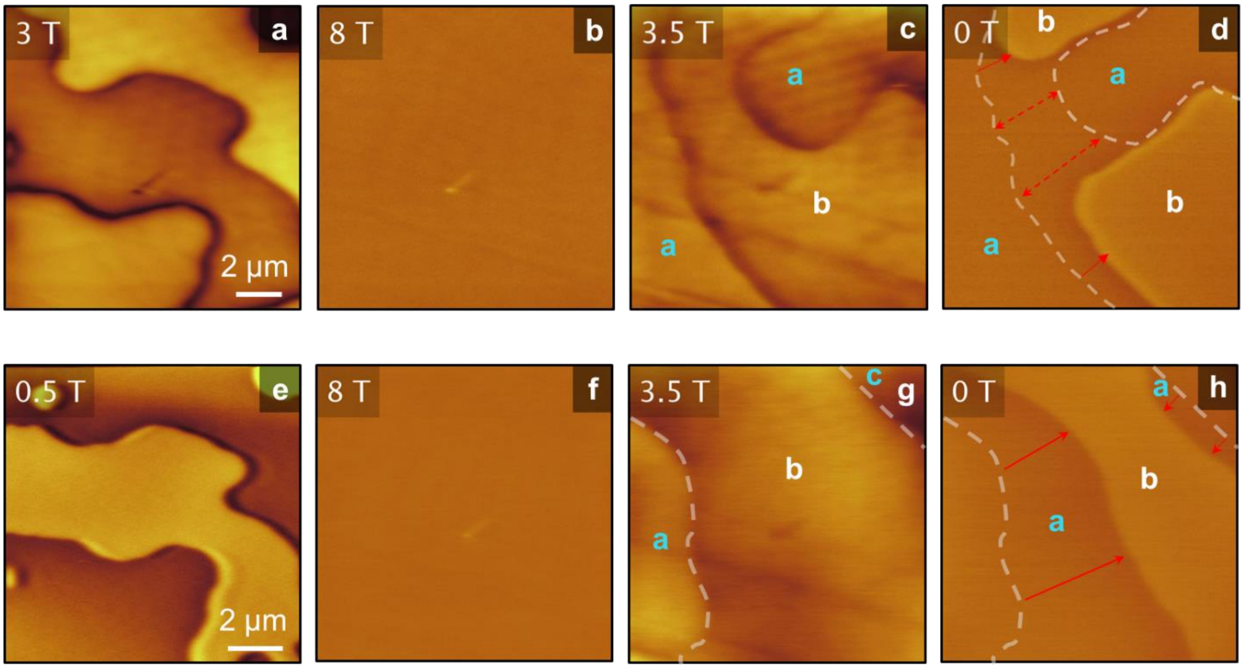

Figure S15. (a-d) MFM images from Figure 3 showing additional scan at 8 T in the saturated state. (e-h) Additional MFM images at 6 K (after resetting the domain state with thermal cycling above T_N) with decreasing magnetic field beginning at a field lower than the spin-flop transition (e). (g) Randomly nucleated DWs appear upon reentry into the canted AFM state after coming down from the saturated state (f). The two AFM phases are labelled **a** and **b**. (h) In the AFM state, the DWs creep, indicated by solid red arrows, inward to form a smaller domain b, a process similar to that in (d). The color scale for the MFM images is 1 Hz (a-d) and 0.5 Hz (e-h).